Asian Journal of Chemistry; Vol. 26, No. 13 (2014), 4133-4139

ASIAN JOURNAL OF CHEMISTRY

http://dx.doi.org/10.14233/ajchem.2014.17732

Manufacturing of C_f/SiC Composites through Combined CVI and High-Pressure PIP Process†

Dong Won Im[1], Tae-Eon Kim[2], Jin Chul Bae[2], Kwang Yeon Cho[2,*], Jung Sup Lim[1] and Jung Il Kim[1]

[1]DACC Co., Ltd., Palbok-dong 2-ga, Deokjin-gu, Jeonju-si, Jeonbuk, Republic of Korea
[2]Nano Convergence Intelligence Materials Team, The Korea Institute of Ceramic Engineering and Technology, 233-5, Gasan-dong, Geumcheon-gu, Seoul, Republic of Korea

*Corresponding author: Fax: +82 2 32827769; Tel: +82 2 32827776; E-mail: kycho@kicet.re.kr

Published online: 23 June 2014; AJC-15427

Carbon fiber-reinforced SiC matrix (C_f/SiC) composites were fabricated using a chemical vapor infiltration + polymer infiltration and pyrolysis (CVI+PIP) hybrid process. In an effort to improve the yield of SiC pyrolyzed during PIP, we conducted pyrolysis under high pressure using polycarbosilane as a precursor. We investigated the effects of the high-pressure pyrolysis of the polycarbosilane infiltrate on the efficiency of the PIP process and the physical characteristics of the fabricated C_f/SiC composites. The CVI+PIP hybrid process under high-pressure pyrolysis reduced the processing time by a factor of ten, minimized the oxygen content (< 10 at %) and improved the crystallinity of the nano β-SiC crystal. These results are due to the pressure in the polycarbosilane pyrolysis, which resulted in a high polycondensation. The ceramic yield of polycarbosilane infiltrated into C_f-preform was increased and the inter-facial bonding between the matrix and fibers was improved. Consequently, the C_f/SiC composites fabricated by the CVI+PIP hybrid process under high-pressure pyrolysis exhibited a high density of 2.15 g/cm^3.

Keywords: Carbon fiber, Silicon carbide, Ceramic matrix composites, Polycarbosilane, Nano β-SiC crystal.

INTRODUCTION

Carbon fiber-reinforced silicon carbide (C_f/SiC) composites are a type of ceramic matrix composites (CMCs) that have many potential applications, such as high-temperature structural components, owing to their outstanding mechanical properties, including high strength at elevated temperatures, low weight (due to their low density) and high toughness[1]. The C_f/SiC composites are manufactured by densely filling the voids within a preform produced from carbon fibers with SiC. To densify a C_f preform, various techniques are employed, such as chemical vapor infiltration (CVI)[2-6], hot pressing (HP) and polymer infiltration and pyrolysis (PIP)[7-9]. Liquid silicon infiltration (LSI) would be the most economical and efficient process. But, LSI process cannot be used in the severe condition of high temperature (T = 2000 ºC) due to free silicons creating in the matrix at temperature above 1400 ºC. The most common process for synthesizing C_f/SiC composites that is available for severe condition is chemical vapor infiltration (CVI). The SiC matrix synthesized by this process displays excellent C_f/SiC interfacial bonding, with the stoichiometric C:SiC ratio being nearly 1:1. Nevertheless, the high production costs and long processing time of CVI pose limitations to its application. Therefore, PIP has recently been extensively studied owing to its lower processing temperature, shorter processing time and use of simple production equipment[10]. Polymer infiltration and pyrolysis is a process for synthesizing C_f/SiC composites *via* pyrolysis after infiltrating a porous C_f-preform with a liquid polymeric precursor, such as polycarbosilane (PCS), polymethylsilane (PMS), or hexamethyldisilazane (HMDS)[11]. However, the C_f/SiC composites synthesized by PIP have a weak C_f/SiC interfacial bonding, which is ascribed to the pyrolysis-induced shrinkage of the infiltrated polymeric precursor (polycarbosilane in the present case). Moreover, cracks can be propagated into the matrix of the composites if the pyrolysis is repeatedly performed. Furthermore, undesired oxygen (O) enters and diffuses during repeated pyrolysis and triggers the formation of a SiC matrix phase with the composition Si-O-C that substantially lowers the mechanical properties of the composite at temperatures exceeding 1300 ºC[12,13]. In recent years, to overcome these drawbacks, hybrid techniques combining CVI and PIP have been developed to synthesize C_f/SiC composites. In a CVI+PIP hybrid process, the interfacial bonding between the carbon fibers and SiC matrix is strengthened by CVI and the voids are filled by the SiC matrix in the subsequent PIP. This hybrid process can improve the

†Presented at 5th International Symposium on Application of Chemical and Analytical Technologies in Nuclear Industries (Nu-ACT 2013), Daejeon, Korea

mechanical properties of the C_f/SiC composites and minimize the processing time and cost. Further, the efficiency of this hybrid process mainly depends on minimizing the number of PIP cycles and the amount of oxygen diffused during PIP.

Against this backdrop, the present study is aimed to facilitate the manufacturing process of C_f/SiC composites to improve their mechanical properties using a CVI+PIP hybrid process. Additionally, in an effort to improve the yield of SiC pyrolyzed during PIP, we conducted the pyrolysis under high pressure, resulting in reduced processing time, minimized diffusion of oxygen and improved crystallinity of β-SiC. Next, we evaluated the densification behaviour of the high-pressure CVI+PIP hybrid process depending on the number of process cycles. Furthermore, we evaluated the mechanical properties of the synthesized C_f/SiC composites and we observed the microstructure of the fracture surfaces to analyze the fracture behaviour of the matrix.

EXPERIMENTAL

Raw materials: Fig. 1 shows the cross-sectional microstructure of the C_f-preform used for the reinforcement of the C_f/SiC composites. The C_f-preform was produced by the needle punching process, wherein carbon fibers were arrayed in the x/y axial directions by cross-stacking them in the 0º/90º directions and needling was performed perpendicular to the x/y plane to achieve a quasi-3D structure, with the carbon fibers aligned along the z-axis. The properties of the C_f-preform are listed in Table-1. Polycarbosilane was used as a polymer precursor to infiltrate the C_f-preform; its mean molecular weight and melting point were 1400 and 161 ºC, respectively. Table-2 outlines the properties of the polycarbosilane.

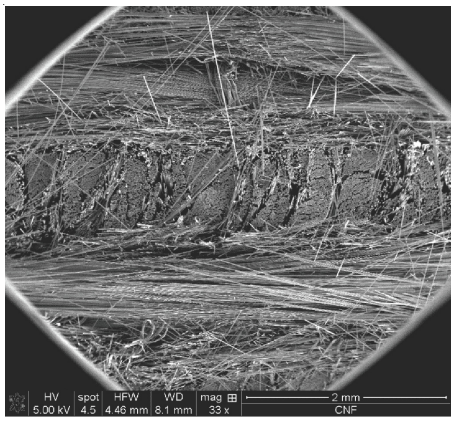

Fig. 1. Cross-sectional image of carbon fiber preform with Quasi-3D structure

TABLE-1
CHARACTERISTICS OF CARBON FIBER PREFORM FOR REINFORCEMENT OF C_f/SiC COMPOSITES

Materials	Density (g/cm^3)	Fiber volume (vol %)	Stacking angle (º)	Company
Carbon fiber	0.55	30	0/90	CNF

TABLE-2
CHARACTERISTICS OF POLYCARBOSILANE (PCS) USED IN PIP PROCESS

Materials	Mw (Daltons)	m.p. (ºC)	Ceramic yield (%)	Company
PCS	1400	161	33	ToBeM tech

Synthesis of C_f/SiC composites: In this study, we used the C_f-preform as a reinforcing material, made by CNF Co., Ltd. The C_f-preform was densified with SiC matrix through the CVI+PIP hybrid process. Additionally, to improve the mechanical properties of the C_f/SiC composites, we generated an interface layer by depositing pyrolytic carbon (Py.C) on the carbon fiber surface.

The C_f-preform was inserted into an isothermal-isobaric reactor and Py.C was deposited by thermal decomposition of propane (C_3H_8) gas. After depositing Py.C, the C_f-preform was cooled down to room temperature. Subsequently, methyltrichlorosilane (CH_3SiCl_3) and H_2 gases mixed in a ratio of 1:20 were introduced into the C_f-preform to deposit the SiC matrix using a different reactor. To achieve a homogeneous deposition of SiC inside the C_f-preform, pressure-gradient CVI was employed. Fig. 2 shows a schematic of the CVI device employed for homogeneous SiC deposition. The blue line with solid arrows in the figure represents the direction of the reactant gas flow. As demonstrated in the figure, the reactant gas was supplied through the lower part of the CVI device and released from the inside of the C_f-preform to the outside. At this instant, the pressure within the reactor was sustained at the process pressure (20 torr) using a vacuum pump installed outside the reactor chamber. The pressure inside the C_f-preform (to which the raw gas was supplied) was maintained at a higher level than the pressure outside the preform (from which the raw gas was released), thereby generating a pressure gradient in the thickness direction of the C_f-preform. Table-3 outlines the deposition conditions for the Py.C interface layer and the SiC matrix.

TABLE-3
DEPOSITION CONDITIONS OF Py.C AND SiC MATRIX

Deposition Material	Temp. (ºC)	Pressure (torr)	Deposition time (h)	Reaction gas	Total flow rate (sccm)
Py.C	1020	20	10	C_3H_8	700
SiC	980	20	72	CH_3SiCl_3, H_2	3000

The voids within the C_f-preform were partly filled with SiC during CVI and PIP was performed to produce high-density C_f/SiC composites. First, polycarbosilane was inserted into a graphite crucible with an inner diameter of 30 mm × 30 mm, whereupon the porous C_f-preform with the Py.C layer and SiC matrix was placed. The graphite crucible containing the polycarbosilane and C_f-preform was then placed inside a reactor capable of heating under vacuum and the polycarbosilane was melted by heating it to 300 ºC under a reduced pressure of 375 mm Hg. To increase the infiltrated contents of polycarbosilane into the C_f-preform, the melted polycarbosilane was kept at 300 ºC for 6 h. The reactor was then cooled down to room temperature and the vacuum was released. Next, the C_f-preform infiltrated with polycarbosilane, which solidified after cooling, was retrieved and placed on a sieve. Iodine was placed on the bottom plate of this sieve and the closed sieve was then placed in a drying oven under a nitrogen atmosphere. A temperature of 120 ºC was maintained for 6 h to cure the polycarbosilane in the C_f-preform through sufficient gasification of iodine. The C_f-preform infiltrated with cured polycarbosilane was then placed in a heat-treatment furnace under an

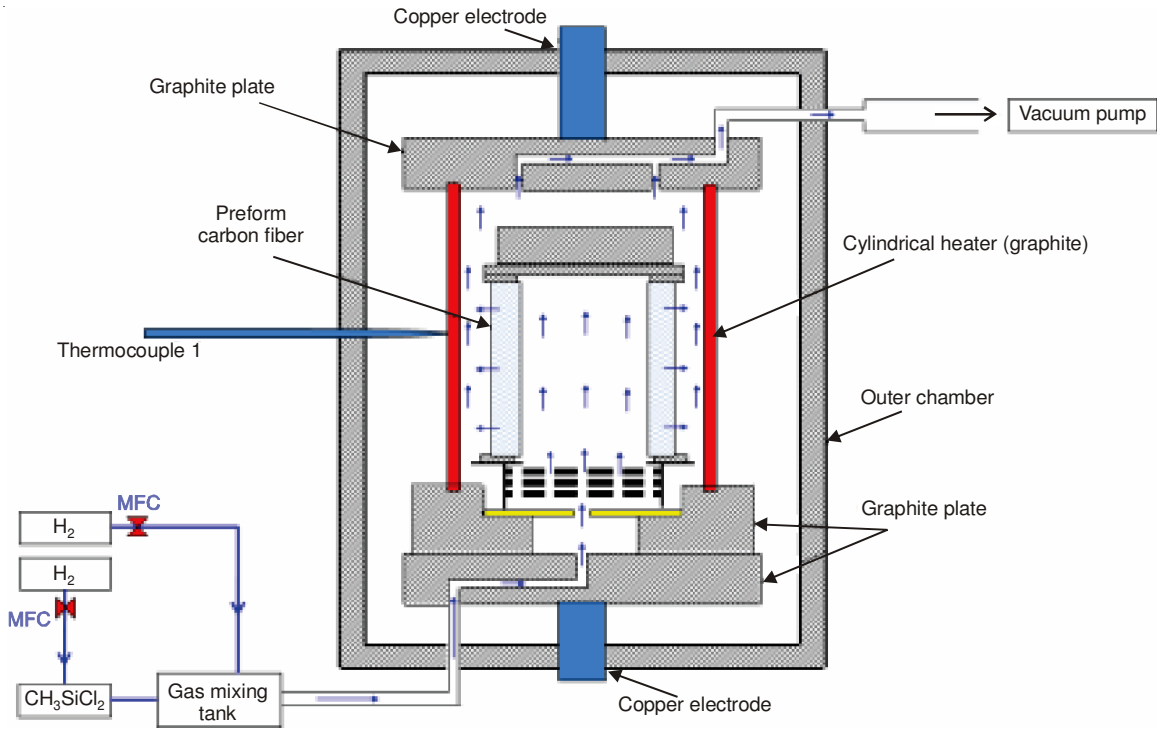

Fig. 2. Schematic of pressure gradient CVI reactor to densify SiC matrix

inert atmosphere (Ar gas) and heated at a rate of 10 ºC/min to a temperature of 1300 ºC and this temperature was maintained for 3 h to sufficiently pyrolyze the polycarbosilane and convert it to a ceramic. The processes of infiltration, curing and pyrolysis were repeated several times to increase the density of the C_f/SiC composites. After the infiltration process was repeated five times, to boost the densification rate, pyrolysis was performed under an interior pressure exceeding 500 bar *via* heat treatment up to 1300 ºC in an Ar environment that was generated using a high-pressure compressor. This infiltration process supported by high-pressure pyrolysis was performed three times, whereby the C_f-preform infiltrated with polycarbosilane was unaffected by the curing process. This is because polycarbosilane, although melted during the high-pressure pyrolysis, did not flow out of the C_f-preform because of the high pressure. The whole process to get the completely densified C_f/SiC composites from the C_f-preform required about 165 h.

Characterization: The process efficiency of manufactured C_f/SiC composites was analyzed by apparent density. The apparent density (five specimens of cylinder type: diameter 7.8 mm, thickness 10 mm) was measured by the Archimedes's law method (ASTM C1039-85) calculating average value. Microstructure and porosity were investigated by cross-section and fracture surface for the densification behaviour of the manufactured C_f/SiC composites. Microstructure of the specimens was observed by scanning electron microscope (SEM, Hitachi S-4800). Cross-section image, 20 mm (width) × 15 mm (length) × 7 mm (thickness) was observed after polishing and the fracture surface image was observed at rupture surface after measuring tensile strength. The porosity was investigated by porosimeter (Micromeritics, Autopore III 9400). To observe the pore size associated with impregnation of C_f/SiC composites, active pore size was distributed. The specimen size has diameter of 7.8 mm and thickness of 10 mm. Moreover, in order to evaluate mechanical properties of the manufactured C_f/SiC composites, tensile strength and shearing strength were measured by ASTM C1275 and ASTM C1292 method, respectively. The shape of the specimen for tensile strength and shearing strength tests was bar type (width 6 mm × length 100 mm × thickness 3 mm and width 15 mm × length 30 mm × thickness 6 mm), Notch with 3 mm depth was engraved being interlaced on the front and back. In addition, to evaluate the mechanical properties, universal test machine (Instron, Instron 5582) was used by test condition in crosshead displacement rate of 1 mm/min and measured data on 10 specimens were averaged. Furthermore, crystalline state and chemical composition were analyzed by X-ray diffraction (XRD, Rigaku Miniflex) and X-ray photoelectron spectroscope (XPS, Thermo VG, K-alpha).

RESULTS AND DISCUSSION

Fig. 3 shows a graph depicting the changes in the density of the C_f-preform with respect to the infiltration method and the number of times it was performed. Chemical vapour infiltration increased the C_f-preform density from 0.55 to 1.26 g/cm^3; the density was further increased up to 1.63 g/cm^3 after five PIP cycles accompanied by atmospheric-pressure pyrolysis. The density hardly increased after the fifth cycle of atmospheric-pressure PIP. After that, a further increase in the density was achieved by additional PIP cycles accompanied by high-pressure pyrolysis, ultimately resulting in a density of 2.15 g/cm^3 for the C_f/SiC composites. The first cycle of high-pressure PIP showed excellent densification efficiency by abruptly boosting the C_f-preform density from 1.63 to 1.95 g/cm^3. The final C_f/SiC composite density of 2.15 g/cm^3 was achieved after performing three cycles of high-pressure PIP. The dramatic increase in the densification efficiency *via* high-pressure PIP is presumably

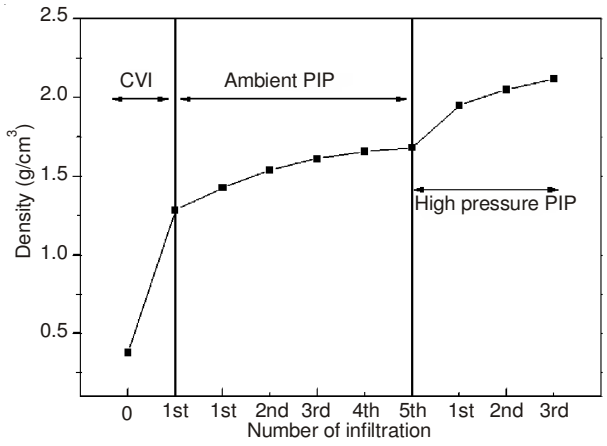

Fig. 3. Increasing of the C_f-preform density as a function of infiltration process

attributable to the sharp increase in the ceramic yield obtained from the polycarbosilane conversion after pyrolysis and to the concurrent retention of polycarbosilane infiltrated by volatile gas within the C_f-preform by enclosing the melted polycarbosilane.

Fig. 4(a) and (b) show the cross-sectional microstructure of the C_f/SiC composites synthesized under atmospheric- and high-pressure conditions, respectively. The C_f/SiC composites fabricated *via* atmospheric-pressure PIP contain a relatively large number of pores several hundred micrometers in size. These large pores were mostly observed in the inter-bundle areas rather than the intra-bundle areas and the inter-layer regions between the carbon fibers stacked in the 0°/90° directions. However, the observation of the interior of the C_f/SiC composites manufactured *via* high-pressure PIP revealed that the size and quantity of the inter-bundle and inter-layer pores in the composites were considerably reduced. In particular, most of the inter-layer pores were removed. The results of the pore distribution analysis performed using a mercury porosimeter clearly supported the above observation.

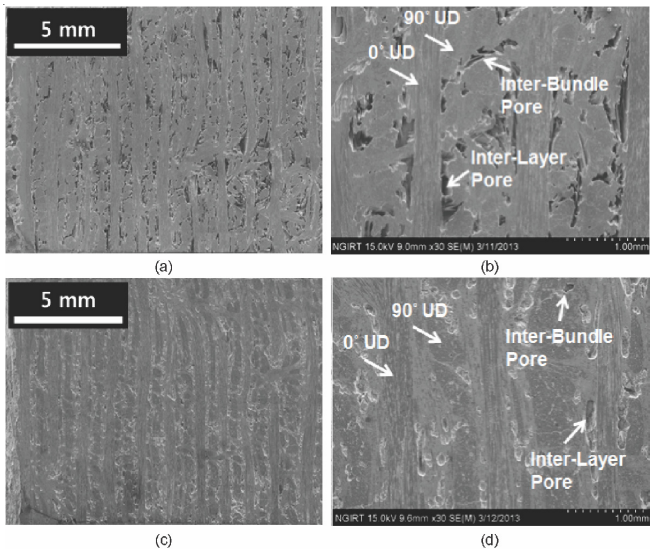

Fig. 4. Cross-sectional images of C_f/SiC composites densified under different pressure condition;(a) ambient pressure, (b) high pressure

Fig. 5 shows pore size distributions of C_f/SiC composites manufactured under different pressure condition in the PIP process. The pore size distributions of C_f/SiC composites *via*

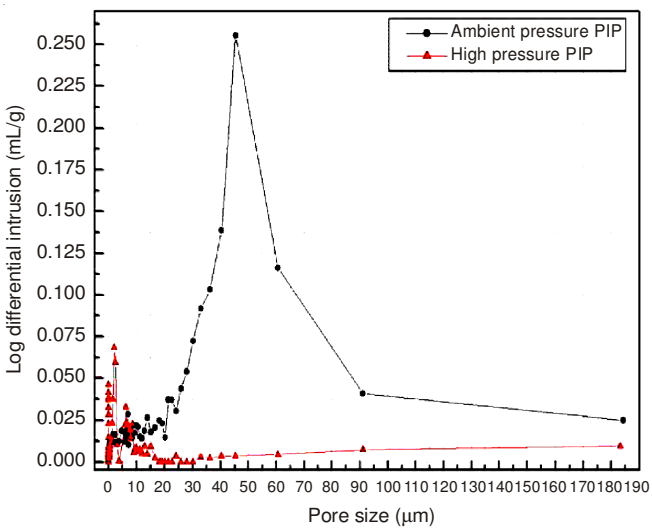

Fig. 5. Pore size distribution of C_f/SiC composites manufactured under different pressure condition PIP process

ambient-pressure pyrolysis were varying from several tens to several hundreds of micrometers as observed in the inter-layer and inter-bundle regions in Fig. 4. On the other hand, the distributions of C_f/SiC composite *via* high-pressure pyrolysis in the figure showed that the size of most post-densification inner pores were smaller than 10 μm. Pores with sizes from several tens to several hundreds of micrometers were estimated to have a very small distribution range. It is because these pores were efficiently filled by the high yield ceramics *via* the conversion of polycarbosilane during the high-pressure pyrolysis.

As shown in Fig. 6(b), the C_f/SiC composites in this study consisted of a Py.C interface layer generated by depositing propane gas pyrolyzed at 1020 °C on the C_f surface, a SiC matrix deposited from thermal decomposition of MTS gas at 980 ºC (CVI-SiC_m) and a SiC matrix densified by pyrolysis after polycarbosilane infiltration (PIP-SiC_m). Specifically, the C_f/SiC composites were densified up to 2.15 g/cm^3 *via* high-pressure PIP after the deposition of SiC *via* CVI (Fig. 6(a)). The composites were densely filled with CVI-SiC_m and PIP-SiC_m, except for a small number of micropores (several micrometers in size) present in the intra-bundles. Furthermore, the analysis of the inter-bundle areas, in which relatively large pores were found, also confirmed a homogeneously densified structure.

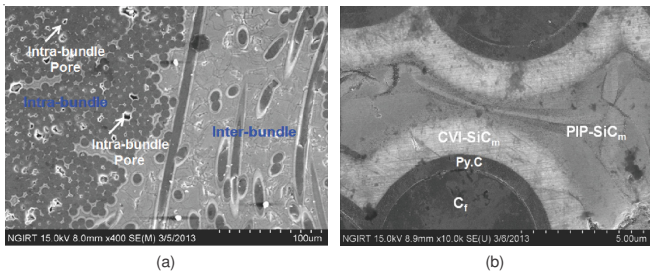

Fig. 6. Microstructure of C_f/SiC composites reinforced with carbon fiber. (a) Intra- and inter-bundle pores were filled with CVI-SiC_m and PIP-SiC_m. (b) Py.C interface deposited on carbon fiber surface

Fig. 7 depicts the tensile and shear strength of the C_f/SiC composites. The C_f/SiC composites densified *via* CVI and high-pressure PIP showed a tensile strength of 195 MPa and a shear

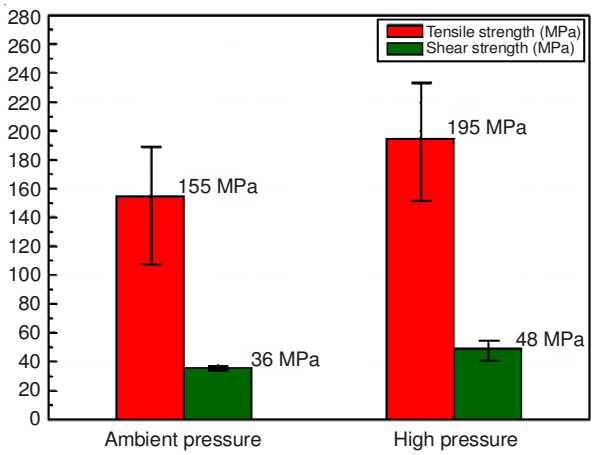

Fig. 7. Mechanical properties of C_f/SiC composites as a pressure of PIP process

strength of 48 MPa. These values are significantly higher than those for the C_f/SiC composites densified *via* CVI and atmospheric-pressure PIP. This is attributable to the fact that the drastic increase in the pyrolytic yield of polycarbosilane induced by high-pressure pyrolysis. In other words, generation of micro sized cracks from the contraction in the thermal decomposition of polycarbosilane was significantly reduced in matrix. Lowered the frequency of microcrack formation and simultaneously resulted in the high densification of the composite microstructure by densely filling the inter- and intra-bundle gaps with SiC. Therefore, according to the Griffith's theory on the relation between defect (cracks and pores) size and the fracture strength, the manufactured C_f/SiC composites were expected to have high-strength by the relatively small pore and high-pressure thermal decomposition (Fig. 5).

The images in Fig. 8 show the microstructure of the fracture surfaces obtained after the tensile test of the C_f/SiC composites. The fracture surfaces showed some pullouts of the carbon fiber bundles and filaments from the SiC matrices. The C_f/SiC composites densified *via* CVI and high-pressure PIP showed a higher number of carbon fiber filament pullouts than the C_f/SiC composites densified *via* CVI and atmospheric-pressure PIP. This observation may be attributed to the presence of the many pores within the inter-bundle area, due to the incomplete filling of pores by SiC converted from polycarbosilane in the case of the C_f/SiC composites densified *via* CVI and atmospheric-pressure PIP (Fig. 4(a)) and due to the difficulty in the generation of individual carbon fiber pullouts from the matrices when fracture occurs.

Fig. 9 shows the strength-displacement curves for the C_f/SiC composites. Both fracture curves show fracture behaviour typical of C_f/SiC composites[8,14-17]. The C_f/SiC composites were completely fractured after experiencing matrix cracking, matrix-fiber debonding and crack deflection and fiber pull-out[15,16]. Linear elastic region shortly appeared at the beginning. Ubeyli *et al.*[17] reported that if the thickness of the interface layer increases, the damage tolerance also increase[14,16-18]. Likewise, Fig. 6 shows that the damage tolerance highly increases, as the thickness of the interface layer becomes 2.5 μm. Increase of the strength value was contributed to the fiber pull-out shortly before the highest fracture strength and this result was clearly shown in Figs. 10 and 11.

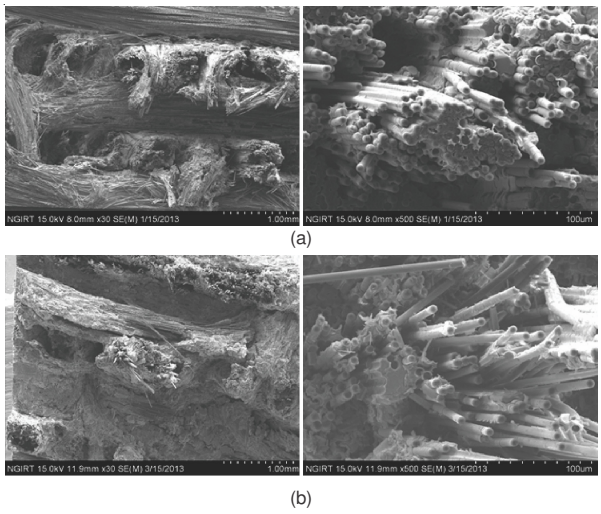

Fig. 8. Fracture surface images of C_f/SiC composites manufactured under different pressure condition; (a) ambient pressure, (b) high pressure

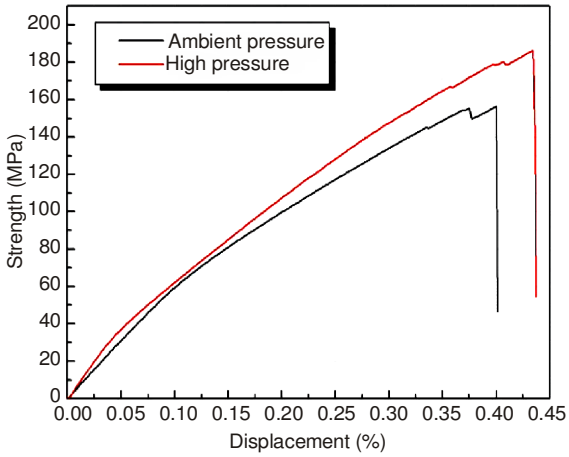

Fig. 9. Strength-displacement curves of C_f/SiC composites manufactured under different pressure condition

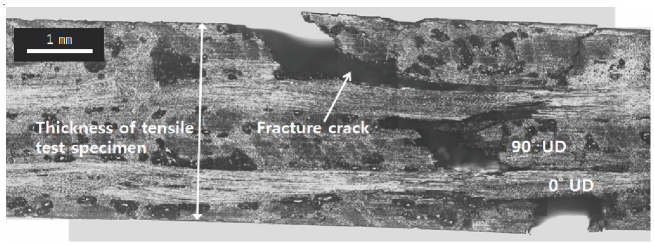

Fig. 10. Cross-sectional image of tensile test specimen reveals a path of a fracture crack

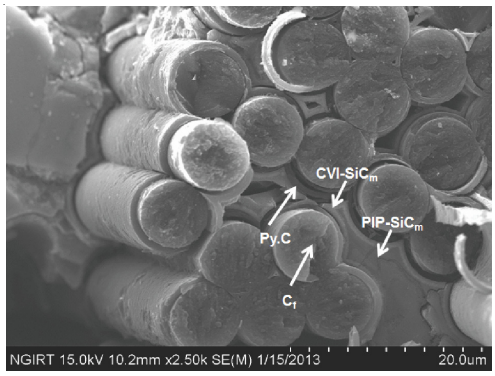

Fig. 11. Fracture surface image of C_f/SiC composites reveals quasi-ductile fracture with help of Py.C interface between carbon fiber and SiC matrix

The strength and strain values for the C_f/SiC composites densified *via* the CVI and high-pressure PIP process were higher than those for the C_f/SiC composites densified *via* the CVI and the atmospheric-pressure PIP process.

Figs. 10 and 11 show SEM images of the microstructure of the C_f/SiC composites synthesized *via* the CVI + PIP hybrid high-pressure process exhibiting quasi-ductile fracture behaviour. The image in Fig. 10 shows the fracture crack path propagating along the specimen thickness as a result of the tensile test. An abrupt change in the fracture crack propagation path takes place in the carbon fiber area (0º UD) aligned perpendicularly to the thickness direction of the specimen during the tensile test and a fracture crack is observed to propagate relatively easily along the 0º and 90º UD inter-layer regions having a relatively low volume fraction of carbon fibers. A fracture crack initiated in the SiC matrix because of external stress does not propagate directly from the SiC matrix to the carbon fibers, but along the interface between the carbon fiber and the matrix. This phenomenon is demonstrated by carbon fibers sliding from their interface with the matrix, resulting in pullouts[15,16,19]. In the microstructure image in Fig. 11, it can be observed that the intra-bundle fracture surface is covered with carbon fibers with irregular heights as a result of the carbon fiber pullouts. Fiber sliding is also observed at the interface between the carbon fiber and the matrix. The Py.C layer deposited on the carbon fibers in this study is estimated to efficiently control the strong interfacial bonding between the SiC matrix and carbon fibers.

Fig. 12(a) shows the X-ray diffraction (XRD) graphs for specimens with polycarbosilane pyrolyzed up to 700 ºC under atmospheric- and high-pressure conditions. Both specimens show an overall amorphous state, with peaks appearing in the vicinities of the (111) and (220) faces, respectively, confirming the formation of β-SiC crystals. The specimen produced through high-pressure pyrolysis showed a relatively high XRD peak intensity, which demonstrates that its crystal phase is better developed. Fig. 12(b) shows the XRD graphs for specimens obtained by additional pyrolysis of polycarbosilane up to 1300 ºC. Both specimens show an overall amorphous state, with peaks appearing on the (111), (220) and (311) faces, confirming the crystal phase development of β-SiC crystals with increasing temperature. Additionally, the specimen that underwent heat treatment under high pressure showed higher peak intensities and the specimen pyrolyzed under high pressure showed a peak corresponding to the (200) face. This is presumably because the pressure exerted during polycarbosilane pyrolysis consolidates the intermolecular bonding and simultaneously increases the quantity of low molecular weight materials that participate in the polycondensation, resulting in the development of a crystal phase. This confirms that the high pressure exerted during polycarbosilane pyrolysis is a very important parameter for the development of β-SiC crystals.

Fig. 13 shows an XPS graph for the polycarbosilane specimen pyrolyzed under high pressure. This specimen consists of 48.0 at % C, 42.5 at % Si and 8.5 at % O, with a C:Si ratio of 1:13, indicating the presence of residual carbon. The low oxygen content of less than 10 at % is indicative of the fact that when

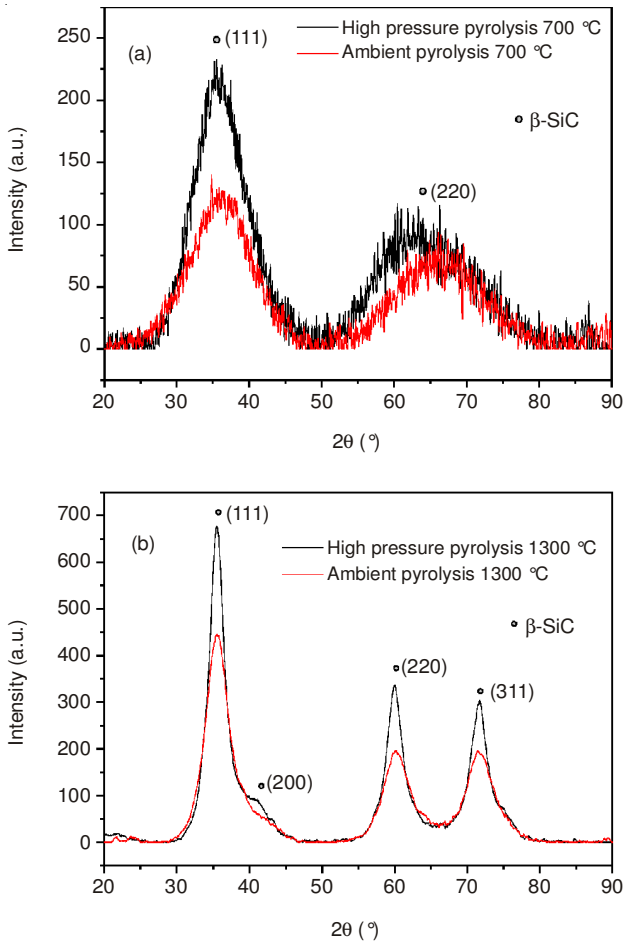

Fig. 12. XRD Patterns of SiC derived from polycarbosilane through ambient, high pressure pyrolysis; (a) pyrolysis 700 ºC, (b) pyrolysis 1300 ºC

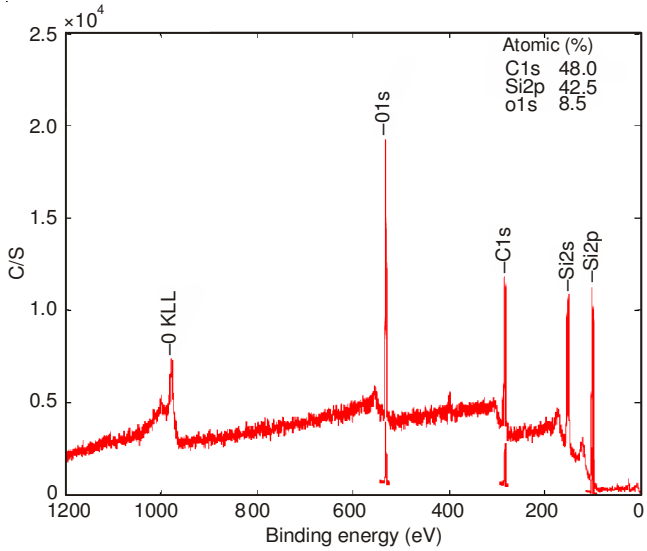

Fig. 13. XPS graph of SiC derived from polycarbosilane through high pressure pyrolysis

polycarbosilane, generally consisting of H, C, Si and O, is pyrolyzed, its volatile constituents such as alcohol and moisture and low molecular weight materials that do not take part in bonding are removed by volatilization. At the same time, a polycondensation reaction takes place, leading to the macroscale growth of a Si-C backbone and thus resulting in the 1:1 bonding ratio of Si and C; the Si-C backbone undergoes

polycondensation during the hydrogen decomposition of CH radicals, ultimately leaving C as residue. Additionally, O, which maintains relatively stronger bonding than hydrogen, survives pyrolysis and tends to bond with atmospheric oxygen during polycarbosilane curing, resulting in an increased O content in the composites. However, the Si-C backbone is formed because of the easy participation of low molecular weight materials in bonding during high-pressure pyrolysis. This is estimated to cause a reduction in the dehydrogenation of atmospheric oxygen during polycarbosilane curing, ultimately leading to a decrease in the oxygen content after final pyrolysis[10].

Conclusion

We produced C_f/SiC composites with a final density of 2.15 g/cm^3 by performing three additional cycles of PIP accompanied by high-pressure pyrolysis. This high-pressure PIP is expected to enhance the ceramic conversion yield of polycarbosilane and simultaneously suppress the exuding of infiltrated polycarbosilane from the matrix in the melted state, thus dramatically boosting the densification efficiency. As a result, the sizes of most of the inner pores of the synthesized C_f/SiC composites were below 10 μm and the majority of the pores in the inter-layer and inter-bundle regions, with sizes ranging from tens to hundreds of micrometers, were removed.

The mechanical strength of the C_f/SiC composites densified *via* CVI and high-pressure PIP was significantly higher than that of the composites densified *via* CVI and atmospheric-pressure PIP. After the fracture test, pullouts of carbon fiber bundles and filaments from the SiC matrix were observed on the fracture surface of the C_f/SiC composites. In particular, more pullouts of carbon fiber filaments were observed in the C_f/SiC composites densified *via* CVI and high-pressure conditions.

The synthesized C_f/SiC composites showed an overall amorphous state. β-SiC crystals were formed in all composites and the composite synthesized by high-pressure pyrolysis of polycarbosilane showed a relatively high XRD peak intensity, thus confirming the development of a crystalline phase. This property is presumably reached because the pressure exerted during the polycarbosilane pyrolysis consolidated the intermolecular bonding and simultaneously increased the quantity of low molecular weight materials participating in the polycondensation, resulting in the development of a crystalline phase.

The composite pyrolyzed under high pressure showed a C:Si ratio of 1:13 and a low oxygen content of less than 10 at %. This ratio is presumably observed because of the formation of a Si-C backbone due to the ready participation of low molecular weight materials in bonding during high-pressure pyrolysis, thus reducing the dehydrogenation of atmospheric oxygen during polycarbosilane curing and ultimately leading to a decrease in the oxygen content after the final pyrolysis.

ACKNOWLEDGEMENTS

This study was sponsored by the Defense Acquisition Program Administration under the contract UC110012GD for the Agency for Defense Development of Key Materials Technology Developments Research Program. We appreciate the assistance of the CNF and ToBeM tech company in fabricating the preforms and polycarbosilane.

REFERENCES

1. E. Fitzer and R. Gadow, *Am. Ceram. Soc. Bull*., **65**, 326 (1986).
2. D.P. Stinton, D.M. Hembree Jr., K.L. More, B.W. Sheldon, T.M. Besmann, M.H. Headinger and R.F. Davis, *J. Mater. Sci*., **30**, 4279 (1995).
3. T. Taguchi, T. Nozawa, N. Igawa, Y. Katoh, S. Jitsukawa, A. Kohyama, T. Hinoki and L.L. Snead, *J. Nucl. Mater*., **329-333**, 572 (2004).
4. T.M. Besmann, J.C. Mclaughlin and H.-T. Lin, *J. Nucl. Mater*., **219**, 31 (1995).
5. T. Noda, H. Araki, F. Abe and M. Okada, *J. Nucl. Mater.*, **191-194**, 539 (1992).
6. K.J. Probst, T.M. Besmann, J.C. McLaughlin, T.J. Anderson and T.L. Starr, *Mater. High Temp*., **16**, 201 (1999).
7. Y.Z. Zhu, Z.R. Huang, S.-M. Dong, M. Yuan and D.-L. Jiang, *J. Inorg. Mater.*, **22**, 954 (2007).
8. A. Kohyama, M. Kotani, Y. Katoh, T. Nakayasu, M. Sato, T. Yamamura and K. Okamura, *J. Nucl. Mater*., **283-287**, 565 (2000).
9. Z. Wang, L. Gao, Y. Ding, B. Wu, H. Zhou, P. He and S. Dong, *Ceram. Int*., **38**, 535 (2012).
10. J.C. Bae, K.Y. Cho, D.H. Yoon, S.S. Baek, J.K. Park, J.I. Kim, D.W. Im and D.H. Riu, *Ceram. Int*., **39**, 5623 (2013).
11. J. Zhong, S. Qiao, G. Lu, Y. Zhang, W. Han and D. Jia, *J. Mater. Process. Technol*., **190**, 358 (2007).
12. Y. Xiang, W. Li, S. Wang, B. Zhang and Z. Chen, *Surf. Coat. Technol*., **209**, 197 (2012).
13. A. Kohyama, M. Kotani, Y. Katoh, T. Nakayasu, M. Sato, T. Yamamura and K. Okamura, *J. Nucl. Mater*., **283-287**, 565 (2000).
14. T.M. Besmann, R.A. Lowden, D.P. Stinton and T.L. Starr, *J. Phys.*, **C5**, 229 (1989).
15. Z. Xu and D. Viehland, *J. Am. Ceram. Soc*., **80**, 2961 (1997).
16. Y. Xu, L. Zhang, L. Cheng and D. Yan, *Carbon*, **36**, 1051 (1998).
17. M. Ubeyli and M. Alkan, *J. Polytech*., **5**, 83 (2002).
18. A. Hasegawa, A. Kohyama, R.H. Jones, L.L. Snead, B. Riccardi and P. Fenici, *J. Nucl. Mater*., **283-287**, 128 (2000).
19. Y. Katoh, L.L. Snead, T. Nozawa, T. Hinoki, A. Kohyama, N. Igawa and T. Taguchi, *Mater. Trans*., **46**, 527 (2005).